microPublication BIOLOGY

10/31/2026 - *Open Access*

A mutation in the conserved NPxY motif of β integrin PAT-3 alters outgrowth of neuronal dendritic spines

Michele L Lemons[1,2§], Noelia Genao[3], Hailey McKillop[3], Michael M Francis[2]

[1]Department of Biological and Physical Sciences, Assumption University, Windsor, ON, Canada

[2]Department of Neurobiology, University of Massachusetts Chan Medical School, Worcester, MA, USA

[3]Department of Biological and Physical Sciences, Assumption University, Worcester, MA, USA

[§]To whom correspondence should be addressed: mlemons@assumption.edu

Abstract

Integrins are heterodimeric transmembrane receptors that are critical in many biological processes, including neuronal development. Here we investigate integrin signaling in the outgrowth of dendritic spines on *C. elegans* GABAergic neurons using mutations engineered within the membrane-distal NPxY motif of the β integrin subunit PAT-3. We found a Y/E substitution, but not Y/A or Y/F substitutions, reduced dendritic spine number and misoriented spines. The Y/E substitution in the NPxY motif also altered the distribution of the presynaptic scaffold CLA-1, suggesting roles in both pre- and postsynaptic development. Our findings implicate integrin activation through the NPxY motif in synapse formation/maturation.

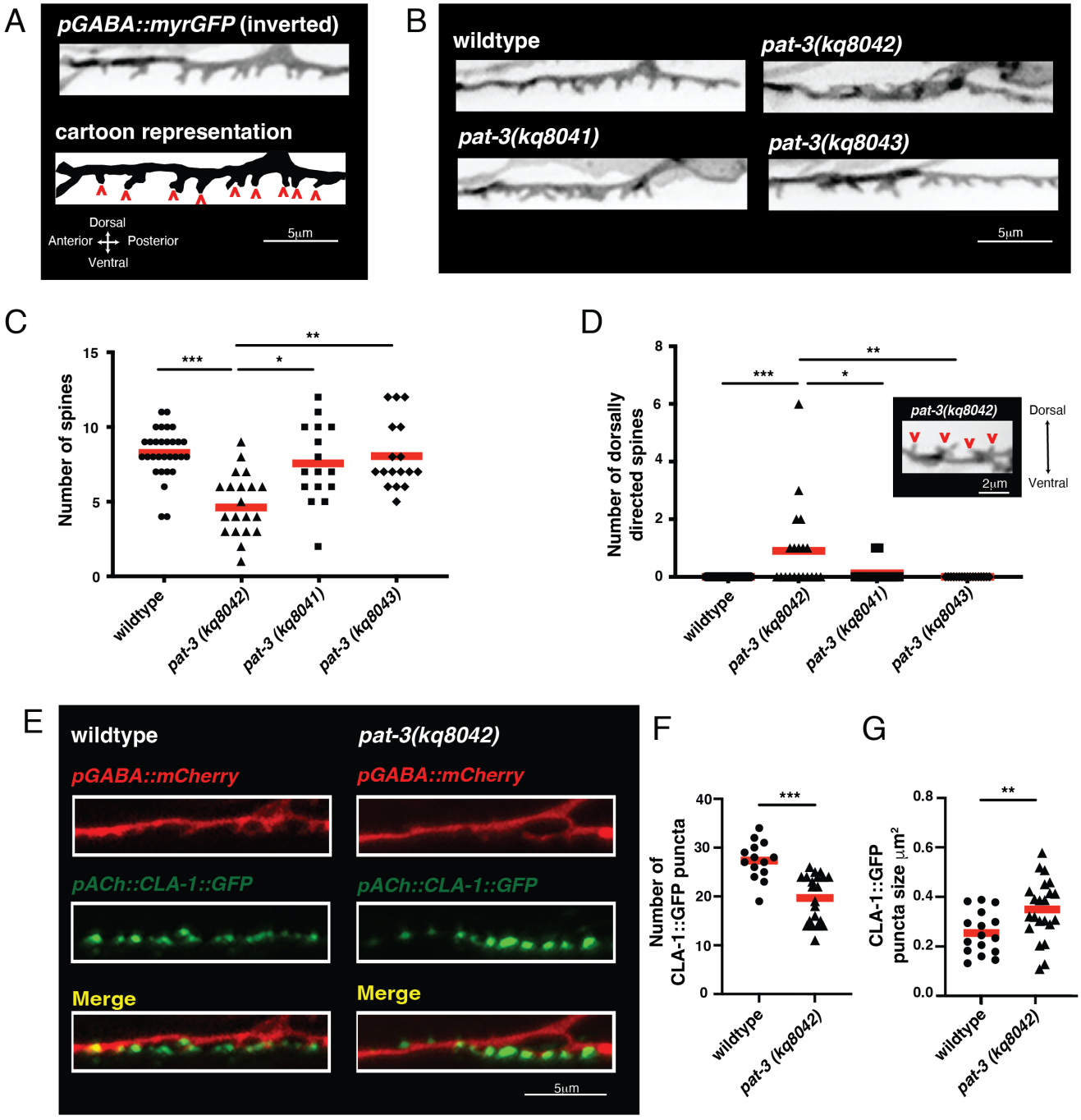

Figure 1. A Y/E substitution in the membrane distal NPxY motif of the cytoplasmic tail of β integrin/*pat-3* disrupts dendritic spines:

A) Maximum projection confocal image of the *C. elegans* GABAergic DD1 neuron dendritic shaft (inverted LUT grey scale) labeled by transcriptional expression of myristoylated GFP (myrGFP). *pGABA*::myrGFP in top image refers to cell specific transcriptional expression of myrGFP in DD GABAergic neurons using the *flp-13* promoter. Bottom panel is a cartoon representation of the top image and includes red carets pointing to ventrally directed spines protruding from the dendritic shaft. All images are from larval stage 4 animals and oriented with anterior to the left and ventral towards the bottom, as indicated by arrows. Scale bar, 5 µm. B) Inverted maximal projection images showing DD1 dendritic spines of wildtype, *pat-3(kq8041)*, *pat-3(kq8042)* and *pat-3(kq8043)* animals. Scale bar, 5 µm. C) Scatterplot of the total number of spines within a 15 µm region of DD1 neurons in wild-type animals and *pat-3* mutants. The number of spines in *pat-3(kq8042)* animals is significantly decreased compared to wildtype, *pat-3(kq8041)*, and *pat-3(kq8043)* animals. Each data point represents a measurement from an independent animal. Red horizontal bar indicates the mean. *p<0.05, **p<0.005, *** p<0.0005, Kruskal Wallis test. D) Number of dorsally directed spines per animal shown as a scatterplot. Dorsally directed spines are significantly increased in *pat-3(kq8042)* compared to wild type. Red horizontal bar indicates the mean. Inset image of *pat-3(kq8042)* animal with carets pointing to dorsally directed spines. *p<0.05, **p<0.005, ***p<0.0005,

Kruskal Wallis test. Scale bar, 2 µm. E) Maximum projection confocal images of *C. elegans* GABAergic DD1 neuron dendritic shaft and spines (red) and presynaptic protein CLA-1 (green). *pGABA*::mCherry refers to transgenic expression of the red fluorescent marker mCherry in GABAergic DD neurons (*flp-13* promoter). *pACh*::CLA-1::GFP refers to expression of the active zone protein CLA-1 tagged with green fluorescent protein (GFP) in cholinergic neurons (*unc-17* beta promoter), including those that are presynaptic to GABAergic DD motor neurons. Representative images of wild type (left) and *pat-3(kq8042)* mutants (right) are shown. Scale bar, 5 µm. Scatterplots showing the average number (F) and size (G) of CLA-1::GFP puncta per animal within a 50 µm anterior most portion of ventral nerve cord. Each dot represents a single animal. The number of CLA-1::GFP clusters is decreased and the size of CLA-1::GFP clusters is increased in *pat-3(kq8042)* animals compared to wild-type controls. ***p<0.0005, **p<0.005, Mann Whitney test.

Description

Synapse formation involves a sequence of carefully orchestrated molecular interactions to concentrate synaptic vesicles and release machinery at precisely defined sites opposite clusters of post-synaptic neurotransmitter receptors (Drapeau et al., 1995; Waites et al., 2005). Many studies have identified shared groups of proteins that form the core pre- and post-synaptic scaffolds, but the events that initiate synapse assembly and maturation often vary at the level of individual neurons and synapses. Mounting evidence indicates that integrin family members have key roles in synapse assembly and maturation (de Wit & Ghosh, 2016; Dityatev et al., 2010; Lilja & Ivaska, 2018; Park & Goda, 2016). Integrins are transmembrane extracellular matrix receptors that function as αβ heterodimers (Campbell & Humphries, 2011; Giancotti & Ruoslahti, 1999; Hynes, 1992, 2002). Integrins bind a variety of ligands including extracellular matrix, cell adhesion and axon guidance proteins, as well as intracellular signaling machinery such as talin and kindlin (Humphries et al., 2006; Moser et al., 2009; Nakamoto et al., 2004; Sonnenberg, 1993; Ye et al., 2014). At least 24 different integrin combinations are formed from 18 α and 8 β subunits in mammals, while the invertebrate model *C. elegans* forms only two integrin heterodimers (Fassler & Meyer, 1995) composed of one α subunit (INA-1 or PAT-2) and a sole β subunit (PAT-3)(Gettner et al., 1995; Kramer, 2005).

Integrin function is greatly influenced by conformational state, integrins shift between low- (inactivated) and high-ligand affinity (activated) states. Integrin activation can be triggered by cytoplasmic signaling, known as “inside-out” activation (Calderwood, 2004a; Ginsberg, 2014; Kim et al., 2011; Liddington & Ginsberg, 2002; Wang, 2012). Inside-out activation is mediated through interactions between phosphotyrosine binding (PTB) domain proteins (including talin, kindlin) and cytoplasmic NPxY (asp-pro-x-tyr) motifs in the β integrin cytoplasmic domain (Bumm et al., 2025; Czuchra et al., 2006; Hanna et al., 2020; Jannuzi et al., 2002; Jannuzi et al., 2004; Kaapa et al., 1999; Lee et al., 2001; Sakai et al., 1998). The cytoplasmic tail of β integrin has two NPxY motifs, the membrane-proximal motif is proposed to interact with talin while the membrane-distal motif has been shown to interact with kindlin (Morse et al., 2014). Tyrosine phosphorylation of the NPxY motifs regulates the binding of PTB domain containing proteins, implicating NPxY motifs as molecular switches for integrin activation and signaling (Bledzka et al., 2010; Calderwood, 2004a, 2004b; Calderwood et al., 2013; Calderwood et al., 2002; Liddington & Ginsberg, 2002). While null mutations in the gene encoding the *C. elegans* β integrin *pat-3* are lethal, viable CRISPR-engineered mutations targeting the membrane-distal NPXY motif of PAT-3 were recently generated (Bumm et al., 2025; Hanna et al., 2020). Building upon previous studies from our lab and others that implicate integrins in the outgrowth of GABAergic axons (Baum & Garriga, 1997; Chisholm et al., 2016; Forrester & Garriga, 1997; Oliver et al., 2019; Poinat et al., 2002), we sought to employ these NPxY engineered mutants to investigate integrin signaling in the formation of previously characterized dendritic spines in *C. elegans* GABAergic neurons (Cuentas-Condori et al., 2019; Lemons et al., 2024; Oliver et al., 2022; Oliver et al., 2026; Philbrook et al., 2018).

To investigate the role of integrin activation through the β integrin/PAT-3 NPxY motif in spine outgrowth, we used cell-specific expression of myristoylated green fluorescent protein (myrGFP) to visualize GABAergic dendrites in 3 available strains carrying CRISPR-engineered mutations in the conserved tyrosine residue of the PAT-3 membrane distal NPxY motif: wild type ^{801}NPVY^{804} to NPVA^{804} [alanine, *pat-3(kq8041)*], NPVE^{804} [glutamate, *pat-3(kq8042)*], or NPVF^{804} [phenylalanine, *(pat-3(kq8043)*] (Bumm et al., 2025; Hanna et al., 2020). These mutations are expected to disrupt the tyrosine residue (A), mimic tyrosine phosphorylation (E), or mimic non-phosphorylatable tyrosine (F), respectively. Consistent with previous studies (Lemons et al., 2024; Oliver et al., 2022; Philbrook et al., 2018), we observed roughly 8 dendritic spines in a 15 µm region anterior to the DD1 GABAergic neuron cell body of wild-type larval stage 4 (L4) animals (Figure 1A-C). The number of dendritic spines on GABAergic DD1 neurons was significantly reduced by 43±6% in *pat-3(kq8042)* animals carrying a Y>E substitution (Figure 1B,C). Surprisingly, some spines appeared dorsally rather than ventrally oriented in these animals (Figure 1B, D), suggesting either misdirected spine growth or the possibility of ectopic synaptic contacts. Substitution of the negatively charged glutamic acid (E) for tyrosine (Y) in *pat-3(kq8042)* animals is predicted to mimic tyrosine phosphorylation (Anthis et al., 2009; Qiu et al., 2019; Reszka et al., 1992).

Previous studies suggest phosphorylation of the distal NPxY motif disrupts kindlin binding, therefore disabling kindlin's ability to co-activate integrin (Bledzka et al., 2010; Harburger et al., 2009). Our findings suggest that constitutive tyrosine phosphorylation disrupts dendritic spines, perhaps by impacting interactions with kindlin/UNC-112 or other modulators of integrin activation that act through this motif.

To ask whether the effects of the PAT-3 Y/E substitution were specific to the post-synapse or affected both pre- and postsynaptic specializations, we examined the distribution of the GFP-tagged active zone marker CLA-1 (Xuan et al., 2017) in cholinergic neurons, which are presynaptic partners to GABAergic motor neurons. As expected, CLA-1::GFP puncta were observed on the ventral side of ventrally directed spines in wild-type controls (Figure 1E), indicating presynaptic specializations opposing the dendritic spines. We found that the number of CLA-1::GFP puncta within a 50 µm region of the anterior ventral nerve cord was significantly decreased in *pat-3(kq8042)* animals compared to controls (Figure 1F), while the size of CLA-1::GFP puncta slightly increased (Figure 1G). These findings demonstrate that both pre- and postsynaptic specializations are disrupted in *pat-3(kq8042)* animals.

We next examined dendritic spines in *pat-3(kq8041)* and *pat-3(kq8043)* animals. A tyrosine (Y) to phenylalanine substitution (F) in the NPxY motif in *pat-3(kq8043)* animals is predicted to preserve hydrophobic interactions associated with tyrosine but eliminate phosphorylation, perhaps acting similarly to a non-phosphorylatable tyrosine residue (Chen et al., 2006; Xu et al., 2010). The tyrosine (Y) to alanine substitution (A) in the NPxY motif of *pat-3(kq8041)* animals is predicted to disrupt interactions requiring the hydrophobic aromatic ring of tyrosine as well as phosphorylation at this site (Chen et al., 2006). Surprisingly, we found that spine number was not significantly different in either of these mutants compared to wild-type animals (Figure 1B,C). Although work to date suggests the membrane-proximal and -distal NPxY motifs have independent binding partners, we can't rule out the possibility that redundancy across the motifs contributes to these findings.

Prior analysis of membrane distal NPxY substitutions revealed that all three substitutions produced defects in the migration of gonadal distal tip cells (Hanna et al., 2020). In contrast, our finding that solely the phosphomimetic Y/E substitution disrupts dendritic spines is more consistent with recent studies of neuronal function in these strains, where the phosphomimetic E substitution produced severe effects, while the A and F substitutions did not (Bumm et al., 2025). Together, our results argue that tyrosine phosphorylation at the distal NPxY motif of PAT-3 is not essential for spine outgrowth, but may instead have a modulatory role, perhaps by influencing integrin interaction with kindlin/UNC-112 (Bledzka et al., 2010; Qadota et al., 2012).

Methods

Strains

All strains used in these experiments are listed in Table 1. Strains are N2 Bristol strain derivatives (wildtype) and were maintained at room temperature on nematode growth media plates seeded with *E. coli* strain OP50. Some strains were kindly shared by the Lee lab at Baylor University (Hanna et al., 2020). Transgenic strains were obtained by microinjection to achieve transformation (Mello et al., 1991) and identified by using co-injection markers. Integrated lines were produced with X-ray irradiation and outcrossed to wild type/N2 Bristol eight times. Only larval stage 4 (L4) hermaphrodites were used in this study.

Confocal microscopy and analysis

Animals were immobilized in sodium azide (0.3 M) on a 2% agarose pad. Images of dendrites of the DD1 neuron shown in Panels A, B and D were obtained using a Yokogawa CSU-10 spinning disk confocal system on an upright Olympus BX51WI microscope equipped with a Hammamatsu C9100-13 EMCCD camera and 63X oil immersion objective. A Cobolt Calypso 491 nm laser was used for excitation, and images were acquired using Volocity 4.3 software (Perkin-Elmer). All images were obtained using identical imaging and laser settings. Z stack volumes were acquired using an objective-coupled Piezo. Image analysis was conducted using Fiji software (open source) as described previously (He et al., 2015; Lemons et al., 2024; Oliver et al., 2022; Philbrook et al., 2018). Briefly, spines that were at least 0.2 µm in length were counted within a 15 µm region of interest (ROI) anterior to the DD1 cell soma.

Images in Panel E were obtained on a Yokogawa CSU-Z1 spinning disk confocal mounted on a Nikon NiE upright motorized microscope equipped with a Nikon 60x oil immersion objective and a Prime BSI Express CMOS camera (Teledyne Vision Solutions). Z stack images were acquired using Nikon Elements software, using identical imaging and

laser settings. CLA-1::GFP puncta number and size were measured within a 50 µm region of the anterior ventral nerve cord using the analyze particles function in Image J.

Reagents

Primers used to confirm *pat-3* (*kq8041*), *pat-3* (*kq8042*) and *pat-3* (*kq8043*).

Forward primer OMF 3153 (primer in Exon 7 *in pat-3* transcript): ggccacagataatgcaacag. Reverse primer OMF3141: (primer in downstream UTR): acaatttatcgctaaatactcgtt. PCR generated 436bp product. Product was sequenced using forward primer OMF3140 (in exon 7): catgatagatccgaatacgc

Table 1. Worm strains

Strain	Genotype	Description	Plasmid	Shortened name
IZ3105	*ufIs175*	DD-specific myristoylated (myr) GFP transcriptional reporter (green)	*ufIs175 [Pflp-13:: myrGFP + Punc-122*::GFP]	*pGABA::myrGFP = ufIs175*
BU8041	*pat-3(kq8041) III*	CRISPR engineered *pat-3* mutation changes NPVY to NPVA (Hanna et al., 2020)		
BU8042	*pat-3(kq8042) III*	CRISPR engineered *pat-3* mutation changes NPVY to NPVE (Hanna et al., 2020)		
BU8043	*pat-3(kq8043) III*	CRISPR engineered *pat-3* mutation changes NPVY to NPVF (Hanna et al., 2020)		
IZ4167	*pat-3(kq8042) III; ufIs175*	DD-specific myrGFP transcriptional reporter (green)	*ufIs175 [Pflp-13:: myrGFP + Punc-122*::GFP]	*pGABA::myrGFP = ufIs175*
IZ4225	*pat-3(kq8042) III; ufIs175*	DD-specific myrGFP transcriptional reporter (green)	*ufIs175 [Pflp-13:: myrGFP + Punc-122*::GFP]	*pGABA::myrGFP = ufIs175*
IZ4226	*pat-3(kq8043) III; ufIs175*	DD-specific myrGFP transcriptional reporter (green)	*ufIs175 [Pflp-13:: myrGFP + Punc-122*::GFP]	*pGABA::myrGFP = ufIs175*
IZ3973	*ufIs128; ufEx1679*	DD-specific mCherry transcriptional reporter (red), extrachromosomal array with cholinergic promoter driving CLA-1::green fluorescent protein (GFP) expression	*ufIs128 [Pflp-13::mCherry+ Plgc-11::mCherry]; ufEx1679 [Punc-17β::GFPnovo2::cla-1 + Plgc-11::GFP]*	*pGABA::mCherry = ufIs128* *pACh::CLA-1::GFP = ufEx1679*

IZ4598	*pat-3(kq8042) III; ufIs128; ufEx1679*	DD-specific mCherry transcriptional reporter (red), extrachromosomal array with cholinergic promoter driving CLA-1::green fluorescent protein (GFP) expression	*ufIs128 [Pflp-13::mCherry+ Plgc-11::mCherry]; ufEx1679 [Punc-17β::GFPnovo2::cla-1 + Plgc-11::GFP]*	*pGABA::mCherry = ufIs128* *pACh::CLA-1::GFP = ufEx1679*

Acknowledgements: We thank Dr. Shankar Ramachandran for technical assistance. We also thank Emily Norman for helpful comments and suggestions.

References

Anthis NJ, Haling JR, Oxley CL, Memo M, Wegener KL, Lim CJ, Ginsberg MH, Campbell ID. 2009. Beta integrin tyrosine phosphorylation is a conserved mechanism for regulating talin-induced integrin activation. J Biol Chem 284(52): 36700-36710. PubMed ID: 19843520

Baum PD, Garriga G. 1997. Neuronal migrations and axon fasciculation are disrupted in ina-1 integrin mutants. Neuron. 19: 51-62. 1047. PubMed ID: 9247263

Bledzka K, Bialkowska K, Nie H, Qin J, Byzova T, Wu C, Plow EF, Ma YQ. 2010. Tyrosine phosphorylation of integrin beta3 regulates kindlin-2 binding and integrin activation. J Biol Chem 285(40): 30370-4. PubMed ID: 20702409

Bumm JH, Lee DD, Qiu Z, Choi AH, Kolluri M, Olsen MJ, Wang L, Lee M. 2025. The beta integrin modulates serotonin sensitivity via NPxY motifs to regulate egg laying and mechanosensation behaviors in Caenorhabditis elegans. Dev Dyn 1442. PubMed ID: 41117756

Calderwood DA. 2004. Talin controls integrin activation. Biochem Soc Trans. 32: 434-7. 675. PubMed ID: 15157154

Calderwood DA. 2004. Integrin activation. J Cell Sci. 117: 657-66. 676. PubMed ID: 14754902

Calderwood DA, Campbell ID, Critchley DR. 2013. Talins and kindlins: partners in integrin-mediated adhesion. Nat Rev Mol Cell Biol 14(8): 503-17. PubMed ID: 23860236

Calderwood DA, Yan B, de Pereda JM, Alvarez BG, Fujioka Y, Liddington RC, Ginsberg MH. 2002. The phosphotyrosine binding-like domain of talin activates integrins. J Biol Chem 277(24): 21749-58. PubMed ID: 11932255

Campbell ID, Humphries MJ. 2011. Integrin structure, activation, and interactions. Cold Spring Harb Perspect Biol 3(3): 10.1101/cshperspect.a004994. PubMed ID: 21421922

Chen H, Zou Z, Sarratt KL, Zhou D, Zhang M, Sebzda E, Hammer DA, Kahn ML. 2006. In vivo beta1 integrin function requires phosphorylation-independent regulation by cytoplasmic tyrosines. Genes Dev 20(8): 927-32. PubMed ID: 16618804

Chisholm AD, Hutter H, Jin Y, Wadsworth WG. 2016. The Genetics of Axon Guidance and Axon Regeneration in Caenorhabditis elegans. Genetics. 204: 849-882. 1406. PubMed ID: 28114100

Cuentas-Condori A, Mulcahy B, He S, Palumbos S, Zhen M, Miller DM 3rd. 2019. C. elegans neurons have functional dendritic spines. Elife 8: 10.7554/eLife.47918. PubMed ID: 31584430

Czuchra A, Meyer H, Legate KR, Brakebusch C, Fässler R. 2006. Genetic analysis of beta1 integrin "activation motifs" in mice. J Cell Biol 174(6): 889-99. PubMed ID: 16954348

de Wit J, Ghosh A. 2016. Specification of synaptic connectivity by cell surface interactions. Nat Rev Neurosci 17(1): 22-35. PubMed ID: 26656254

Dityatev A, Schachner M, Sonderegger P. 2010. The dual role of the extracellular matrix in synaptic plasticity and homeostasis. Nat Rev Neurosci. 11: 735-46. 1242. PubMed ID: 20944663

Drapeau P, Catarsi S, Merz DC. 1995. Signalling synapse formation between identified neurons. J Physiol Paris 89(3): 115-23. PubMed ID: 7581300

Fässler R, Meyer M. 1995. Consequences of lack of beta 1 integrin gene expression in mice. Genes Dev 9(15): 1896-908. PubMed ID: 7544313

Forrester WC, Garriga G. 1997. Genes necessary for C. elegans cell and growth cone migrations. Development. 124: 1831-43. 1053. PubMed ID: 9165130

Gettner SN, Kenyon C, Reichardt LF. 1995. Characterization of beta pat-3 heterodimers, a family of essential integrin receptors in C. elegans. J Cell Biol. 129: 1127-41. 1080. PubMed ID: 7744961

Giancotti FG, Ruoslahti E. 1999. Integrin signaling. Science. 285: 1028-32. 363. PubMed ID: 10446041

Ginsberg MH. 2014. Integrin activation. BMB Rep. 47: 655-9. 1163. PubMed ID: 25388208

Hanna J, Ramani S, Williams T, Anaya R, Campion N, Lopez E, et al., Lee M. 2020. Three alleles in the pat-3 locus of Caenorhabditis elegans: mutations in the membrane-distal NPxY phosphotyrosine motif. MicroPubl Biol. 2020 1441. PubMed ID: 32821887

He S, Philbrook A, Mc Whirter R, Gabel CV, Taub DG, Carter MH, et al., Miller DM. 2015. Transcriptional Control of Synaptic Remodeling through Regulated Expression of an Immunoglobulin Superfamily Protein. Curr Biol. 25: 2541-8. 1161. PubMed ID: 26387713

Humphries JD, Byron A, Humphries MJ. 2006. Integrin ligands at a glance. J Cell Sci. 119: 3901-3. 856. PubMed ID: 16988024

Hynes RO. 1992. Integrins: versatility, modulation, and signaling in cell adhesion. Cell. 69: 11-25.. 97.

Hynes RO. 2002. Integrins: bidirectional, allosteric signaling machines. Cell. 110: 673-87. 865. PubMed ID: 12297042

Jannuzi AL, Bunch TA, Brabant MC, Miller SW, Mukai L, Zavortink M, Brower DL. 2002. Disruption of C-terminal cytoplasmic domain of betaPS integrin subunit has dominant negative properties in developing Drosophila. Mol Biol Cell 13(4): 1352-65. PubMed ID: 11950944

Jannuzi AL, Bunch TA, West RF, Brower DL. 2004. Identification of integrin beta subunit mutations that alter heterodimer function in situ. Mol Biol Cell 15(8): 3829-40. PubMed ID: 15194810

Kääpä A, Peter K, Ylänne J. 1999. Effects of mutations in the cytoplasmic domain of integrin beta(1) to talin binding and cell spreading. Exp Cell Res 250(2): 524-34. PubMed ID: 10413605

Kim C, Ye F, Ginsberg MH. 2011. Regulation of integrin activation. Annu Rev Cell Dev Biol. 27: 321-45. 1152. PubMed ID: 21663444

Kramer JM. 2005. Basement membranes. WormBook: 1-15. PubMed ID: 18050423

Lee M, Cram EJ, Shen B, Schwarzbauer JE. 2001. Roles for beta(pat-3) integrins in development and function of Caenorhabditis elegans muscles and gonads. J Biol Chem. 276: 36404-10. 1167. PubMed ID: 11473126

Lemons M L, McKillop H, Genao N, Francis M M. 2024. The extracellular matrix molecule Collagen XVIII/CLE-1 affects neuronal dendritic spines. MicroPubl Biol 2024: 10.17912/micropub.biology.001331. PubMed ID: 39568805

Liddington RC, Ginsberg MH. 2002. Integrin activation takes shape. J Cell Biol. 158: 833-9. 688. PubMed ID: 12213832

Lilja J, Ivaska J. 2018. Integrin activity in neuronal connectivity. J Cell Sci 131(12): pii: jcs212803. 10.1242/jcs.212803. PubMed ID: 29907643

Mello CC, Kramer JM, Stinchcomb D, Ambros V. 1991. Efficient gene transfer in C.elegans: extrachromosomal maintenance and integration of transforming sequences. EMBO J. 10: 3959-70. 1413. PubMed ID: 1935914

Morse EM, Brahme NN, Calderwood DA. 2014. Integrin Cytoplasmic Tail Interactions. Biochemistry 53: 810-820. DOI: 10.1021/bi401596q

Moser M, Legate KR, Zent R, Fassler R. 2009. The tail of integrins, talin, and kindlins. Science. 324: 895-9. 689. PubMed ID: 19443776

Nakamoto T, Kain KH, Ginsberg MH. 2004. Neurobiology: New connections between integrins and axon guidance. Curr Biol. 14: R121-3. 412. PubMed ID: 14986683

Oliver D, Norman E, Bates H, Avard R, Rettler M, Bénard CY, Francis MM, Lemons ML. 2019. Integrins Have Cell-Type-Specific Roles in the Development of Motor Neuron Connectivity. J Dev Biol 7(3): 10.3390/jdb7030017. PubMed ID: 31461926

Oliver D, Ramachandran S, Philbrook A, Lambert CM, Nguyen KCQ, Hall DH, Francis MM. 2022. Kinesin-3 mediated axonal delivery of presynaptic neurexin stabilizes dendritic spines and postsynaptic components. PLoS Genet 18(1): e1010016. PubMed ID: 35089924

Oliver DB, Ramachandran S, Biswas K, Bénard CY, Doitsidou M, McKillop H, et al., Francis MM. 2026. Genome-wide analysis reveals pathways important for the development and maturation of excitatory synaptic connections to GABAergic neurons. G3 (Bethesda) 16(4): 10.1093/g3journal/jkag028. PubMed ID: 41655250

Park YK, Goda Y. 2016. Integrins in synapse regulation. Nat Rev Neurosci. 17: 745-756. 1226. PubMed ID: 27811927

Philbrook A, Ramachandran S, Lambert CM, Oliver D, Florman J, Alkema MJ, Lemons M, Francis MM. 2018. Neurexin directs partner-specific synaptic connectivity in C. elegans. Elife. 7 1401. PubMed ID: 30039797

Poinat P, De Arcangelis A, Sookhareea S, Zhu X, Hedgecock EM, Labouesse M, Georges Labouesse E. 2002. A conserved interaction between beta1 integrin/PAT-3 and Nck-interacting kinase/MIG-15 that mediates commissural axon navigation in C. elegans. Curr Biol. 12: 622-31. 1055. PubMed ID: 11967148

Qadota H, Moerman DG, Benian GM. 2012. A Molecular Mechanism for the Requirement of PAT-4 (Integrin-linked Kinase (ILK)) for the Localization of UNC-112 (Kindlin) to Integrin Adhesion Sites. Journal of Biological Chemistry 287: 28537-28551. DOI: 10.1074/jbc.M112.354852

Qiu Z, Sheesley P, Ahn JH, Yu EJ, Lee M. 2019. A Novel Mutation in an NPXY Motif of β Integrin Reveals Phenotypes Similar to him-4/hemicentin. Front Cell Dev Biol 7: 247. PubMed ID: 31720287

Reszka AA, Hayashi Y, Horwitz AF. 1992. Identification of amino acid sequences in the integrin beta 1 cytoplasmic domain implicated in cytoskeletal association. J Cell Biol 117(6): 1321-30. PubMed ID: 1376731

Sakai T, Zhang Q, Fässler R, Mosher DF. 1998. Modulation of beta1A integrin functions by tyrosine residues in the beta1 cytoplasmic domain. J Cell Biol 141(2): 527-38. PubMed ID: 9548729

Sonnenberg A. 1993. Integrins and their ligands. Curr Top Microbiol Immunol. 184: 7-35. 1414. PubMed ID: 8313723

Waites CL, Craig AM, Garner CC. 2005. Mechanisms of vertebrate synaptogenesis. Annu Rev Neurosci 28: 251-74. PubMed ID: 16022596

Wang JH. 2012. Pull and push: talin activation for integrin signaling. Cell Res 22(11): 1512-4. PubMed ID: 22777425

Xu X, Ahn JH, Tam P, Yu EJ, Batra S, Cram EJ, Lee M. 2010. Analysis of conserved residues in the betapat-3 cytoplasmic tail reveals important functions of integrin in multiple tissues. Dev Dyn 239(3): 763-72. PubMed ID: 20063417

Xuan Z, Manning L, Nelson J, Richmond JE, Colón-Ramos DA, Shen K, Kurshan PT. 2017. Clarinet (CLA-1), a novel active zone protein required for synaptic vesicle clustering and release. Elife 6: 10.7554/eLife.29276. PubMed ID: 29160205

Ye F, Snider AK, Ginsberg MH. 2014. Talin and kindlin: the one-two punch in integrin activation. Front Med 8(1): 6-16. PubMed ID: 24477625

Funding: This work was supported by a collaborative RUI grant from the National Science Foundation, Division of Integrative Organismal Systems IOS1754986 (M.L.L.) and IOS1755019 (M.M.F.)

Conflicts of Interest: The authors declare that there are no conflicts of interest present.

Author Contributions: Michele L Lemons: conceptualization, investigation, funding acquisition, supervision, writing - original draft, methodology, data curation, formal analysis. Noelia Genao: data curation, visualization, investigation. Hailey McKillop: investigation, validation, visualization, data curation. Michael M Francis: conceptualization, methodology, project administration, supervision, writing - review editing, funding acquisition, investigation, resources.

Reviewed By: Anonymous

Nomenclature Validated By: Anonymous

WormBase Paper ID: WBPaper00070194

History: Received September 2, 2026 **Revision Received** September 21, 2026 **Accepted** October 27, 2026 **Published Online** October 31, 2026 **Indexed** November 14, 2026

Copyright: © 2026 by the authors. This is an open-access article distributed under the terms of the Creative Commons Attribution 4.0 International (CC BY 4.0) License, which permits unrestricted use, distribution, and reproduction in any medium, provided the original author and source are credited.

Citation: Lemons ML, Genao N, McKillop H, Francis MM. 2026. A mutation in the conserved NPxY motif of β integrin PAT-3 alters outgrowth of neuronal dendritic spines. microPublication Biology. 10.17912/micropub.biology.002399